Appl Phys B (2012) 108:319–323
DOI 10.1007/s00340-012-4954-4

Applied Physics B
Lasers and Optics

High-peak-power optically pumped AlGaInAs eye-safe laser at 500-kHz repetition rate with an intracavity diamond heat spreader

Y.-F. Chen · K.W. Su · W.L. Chen · K.F. Huang · Y.F. Chen

Received: 23 November 2011 / Revised version: 1 February 2012 / Published online: 21 March 2012

Abstract We report on a compact efficient high-repetition-rate (>100 kHz) optically pumped AlGaInAs nanosecond eye-safe laser at 1525 nm. A diamond heat spreader bonded to the gain chip is employed to improve the heat removal. At a pump power of 13.3 W, the average output power at a repetition rate 200 kHz is up to 3.12 W, corresponding to a peak output power of 560 W. At a repetition rate 500 kHz, the maximum average power and peak power are found to be 2.32 W and 170 W, respectively.

1 Introduction

High-peak-power high-repetition-rate laser sources have been in demand for the applications in the eye-safe wavelength regime near 1.55-μm such as free-space communication, gas sensing, spectroscopy, and medical treatment. The eye-safe laser sources can be realized in several ways including stimulated Raman scattering (SRS) or optical parametric oscillation (OPO) pumped by the high-peak-power Nd-doped lasers [1–7] and the solid state lasers directly use the Er^{3+}-doped or Cr^{4+}-doped gain media [8–11].

Optically-pumped multiple-quantum-wells (MQWs) semiconductor disk lasers have been developed to provide low-divergence, circular, and high quality nearly-diffraction-limited output beams with flexible choices of emission wavelengths via bandgap engineering [12, 13]. The quaternary alloys lattice matched to InP including InGaAsP and AlGaInAs are developed in the quantum confined structure of the semiconductor lasers for generating the radiation at the NIR region [14–18]. Although the InGaAsP systems were commonly employed in the semiconductor lasers of the NIR region in the early stage [19, 20], the AlGaInAs systems have been verified to have higher conduction band offsets and better carrier confinements. So far, the maximum average output power ever reported for the eye-safe laser based on the AlGaInAs material was found to be 2.6 W at the continuous-wave operation [21].

Recently, the AlGaInAs eye-safe pulsed laser was realized with an actively Q-switched 1.06-μm laser as a pump source [22, 23]. However, the average output power and the pulse repetition rate were restricted to 0.52 W and 20 kHz, respectively, due to the poor heat dissipation from the pump area. Here we report, for the first time to our knowledge, on a high-repetition-rate (100–500 kHz) high-power optically pumped AlGaInAs nanosecond eye-safe laser at 1525 nm with an intracavity diamond heat spreader to enhance the heat removal. We employ an Yb-doped pulsed fiber amplifier to be a pump source for providing various pulse repetition rates. With a pump width of 28-ns at a repetition rate of 200 kHz, the average output power and peak output power under an average pump power of 13.3 W are found to be up to 3.12 W and 560 W, respectively. The maximum average power and peak power at a repetition rate 500 kHz are found to be 2.32 W and 170 W, respectively. The overall slope efficiency is maintained as high as 27.3 % at a pulse repetition rate between 100 and 500 kHz.

2 Experimental setup

Figure 1 shows the experimental configuration of the AlGaInAs MQWs laser at the eye-safe region driven by a

Y.-F. Chen · K.W. Su · W.L. Chen · K.F. Huang · Y.F. Chen (✉)
Department of Electrophysics, National Chiao Tung University, 1001 TA Hsueh Road, Hsinchu 30050, Taiwan
e-mail: yfchen@cc.nctu.edu.tw
Fax: +1-886-35-725230

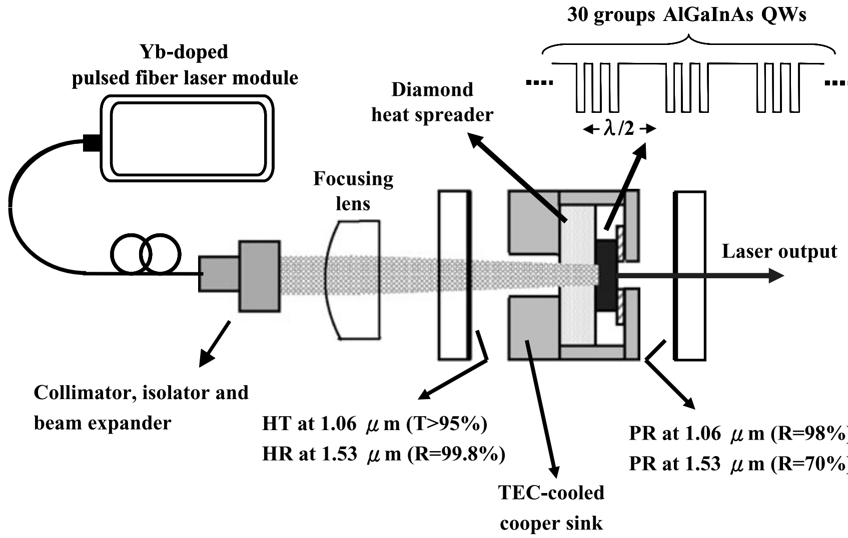

Fig. 1 Experimental setup of AlGaInAs eye-safe laser at 1525 nm with an intracavity diamond heat spreader and using an Yb-doped pulsed fiber amplifier as a pump source

1.06 μm Yb-doped pulsed fiber amplifier (SPI redENERGY G3). The pump source could be operated to provide consecutive pulses with the pulse duration in the range of 9–200 ns and the repetition rate ranging from 10–500 kHz. The pump spot diameter was controlled to be approximately 700 ± 20 μm to have a good spatial overlap with the lasing mode. The laser resonator was designed to be a linear plane-plane cavity which was stabilized by the thermally induced lens of the gain material. The flat mirror at the pump side was coated with antireflection coating at 1.06 μm ($R < 0.2$ %) at the entrance face and with high-reflection coating ($R > 99.8$ %) at 1.53 μm and high-transmission ($T > 95$ %) at 1.06 μm at the other face. The reflectivity of the flat output coupler was 70 % at 1.53 μm. The overall cavity length is approximately 15 mm.

The gain structure is composed of 30 groups of triple QWs spaced at half-wavelength intervals by AlGaInAs barrier layers as shown in the inset of Fig. 1. The thickness of the quantum wells are designed to be 8 nm. The AlGaInAs barriers are only used to separate the QWs not used as strain compensation layers. The resonant-periodic-gain (RPG) structure was designed to locate the QWs at the antinodes of the lasing field standing wave [24, 25]. The periodic AlGaInAs QW/barrier layers were grown on a Fe-doped InP transparent substrate by metalorganic chemical-vapor deposition. The Fe-doped InP transparent substrate with high transmission at the pump and lasing wavelength is used to solve the problem of the lack of good distributed Bragg reflectors (DBRs) for the InP-based systems. The function of conventional DBRs was replaced with an external reflective mirror. A window layer of InP was deposited on the gain structure to prevent surface recombination and oxidation. In contrast to the conventional barrier pumping scheme, the present gain medium was designed to be suitable for in-well pumping to enhance the quantum efficiency [26]. It has been confirmed that the slope efficiency with the in-well pumping scheme was significantly higher than that with the barrier pumping scheme [23]. In the experiment, the single-pass absorption of this gain chip is 81–84 % for repetition rate ranged from 30–500 kHz under 28 ns pump pulse width.

A 4.5-mm square, 0.5-mm thick piece of uncoated single crystal diamond heat spreader was bonded to the MQWs side of the cleaved 2.5-mm square piece of the gain chip to improve the heat removal. Although the heat spreader approach has been used in a variety of high power optically pumped semiconductor lasers [27–29], to the best of our knowledge, the diamond heat spreader is for the first time to be applied to the transparent semiconductor gain medium. The other side of the diamond was in contact with a copper heat sink which was cooled by a thermal-electric cooler (TEC), where the temperature was maintained at 15 °C. The substrate side of the gain chip was attached tightly to a copper plate with a hole of 2-mm diameter, where an indium foil was employed to be the contact interface. The contact uniformity was further confirmed by inspecting the interference fringe coming from the minute gap between the gain chip and the diamond heat spreader. The package configuration of the gain medium can be seen in Fig. 1.

3 Experimental results and discussion

We fixed the duration of pump pulses to be 28 ns for making a detailed comparison at different pulse repetition rates. The spectral information was monitored by an optical spectrum analyzer (Advantest Q8381A) with a diffraction monochromator which could be used for the high-speed measurement of pulsed light with a resolution of 0.1 nm. Figure 2 shows the room temperature spontaneous-emission spectrum of AlGaInAs MQWs pumped with an average absorbed power

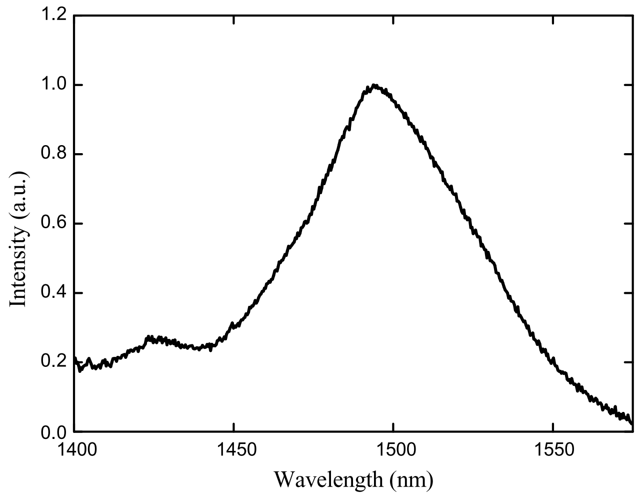

Fig. 2 Room temperature surface emitting spontaneous emission spectrum under a 100-kHz pump repetition rate at an average absorbed power of 0.8 W

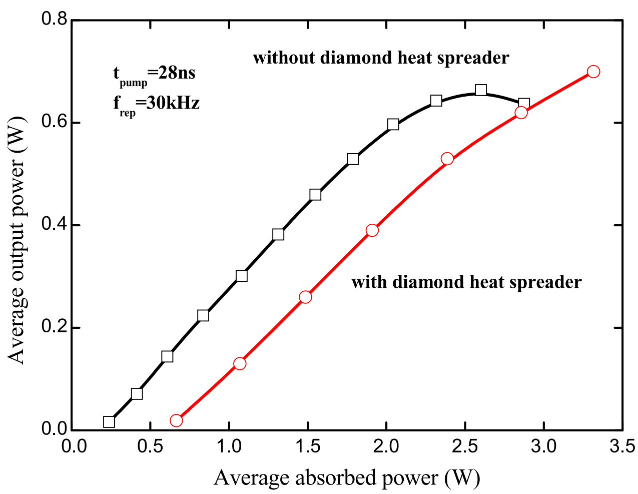

Fig. 3 Output performances of the eye-safe laser without and with the diamond heat spreader at a 30-kHz repetition rate

of 0.8 W at a pulse repetition rate of 100 kHz. It can be seen that the photoluminescence peak at a low pump power was approximately at 1500 nm.

The pump source is a standard commercial product and its maximum output power is dependent on the pulse repetition rate. The maximum output powers of the pump source are approximately 5 W and 20 W for the repetition rates of 30 kHz and 100–500 kHz, respectively. Consequently, we present the experimental results for the laser performance in different figures for the conditions of 30 kHz and 100–500 kHz, respectively. To investigate the losses introduced by the intracavity diamond heat spreader, we make a comparison between the performance of the AlGaInAs eye-safe laser without and with the diamond at the repetition rate of 30 kHz, as shown in Fig. 3. Note that the thermal effect at the repetition rate of 30 kHz is not significant for the absorbed pump power less than 2 W. It can be seen that the output power without the heat spreader displays a thermally induced roll-over effect for the average absorbed power higher than 2.3 W. In contrast, the slope efficiency obtained with the heat spreader can remain nearly constant for the absorbed pump power up to the maximum pump power of 3.3 W, where the maximum pump power is just limited by the pump source at the repetition rate of 30 kHz. This result confirms the improvement of the power scalability by use of the diamond heat spreader. On the other hand, the slope efficiencies obtained without and with the heat spreader can be found to be 33 % and 28 %, respectively. With these slope efficiencies and the output reflectivity of 70 %, the losses introduced by the heat spreader can be estimated to be 7.5 %. Even though there is a room for improving the introduced losses, the diamond heat spreader can extend the operation frequency up to 500 kHz, as shown in the following results.

Figures 4(a) and (b) show the output performances without and with the diamond heat spreader, respectively, for the repetition rate in the range of 100–500 kHz. The maximum average output powers without the heat spreader can be seen to decrease from 0.45 W down to 0.11 W for the repetition rate increasing from 100 kHz to 500 kHz. On the other hand, the average output powers with the heat spreader can be almost maintained linear for the absorbed pump power reaching the maximum value of 13.3 W at the repetition rate within the range of 200–500 kHz. Since the diamond can effectively reduce the thermal effects, the overall beam quality M2 was found to be better than 1.3 for all the pump powers. The maximum average output powers can be found to be up to 3.12 W and 2.32 W for the repetition rates of 200 kHz and 500 kHz, respectively. The roll-over phenomenon observed in Fig. 4(b) for the case of 100 kHz was attributed to the pump-saturation effect. With an absorbed pump power of 10 W and a pump diameter of 700 µm, the pump intensity for the pump duration of 28 ns at 100 kHz could be calculated to be 0.93 MW/cm^2. Since the saturation intensity of the MQW absorption was measured to be approximately within 0.8–1.0 MW/cm^2, the power roll-over phenomenon at 100 kHz was considered to come from the pump-saturation effect.

Figure 5(a) depicts the lasing spectrum with the heat spreader under an average absorbed power of 2.5 W at a repetition rate of 100 kHz. The lasing spectrum can be seen to comprise dense longitudinal modes with the bandwidth to be approximately 10 nm and the center wavelength to be located at 1515 nm. With increasing the average absorbed power, the center wavelength has significant redshifts due to the pump power induced the local heating on the gain medium. Figure 5(b) shows the dependence of the red-shift on the absorbed pump power for the laser operation without and with the heat spreader at a repetition rate of 100 kHz. It

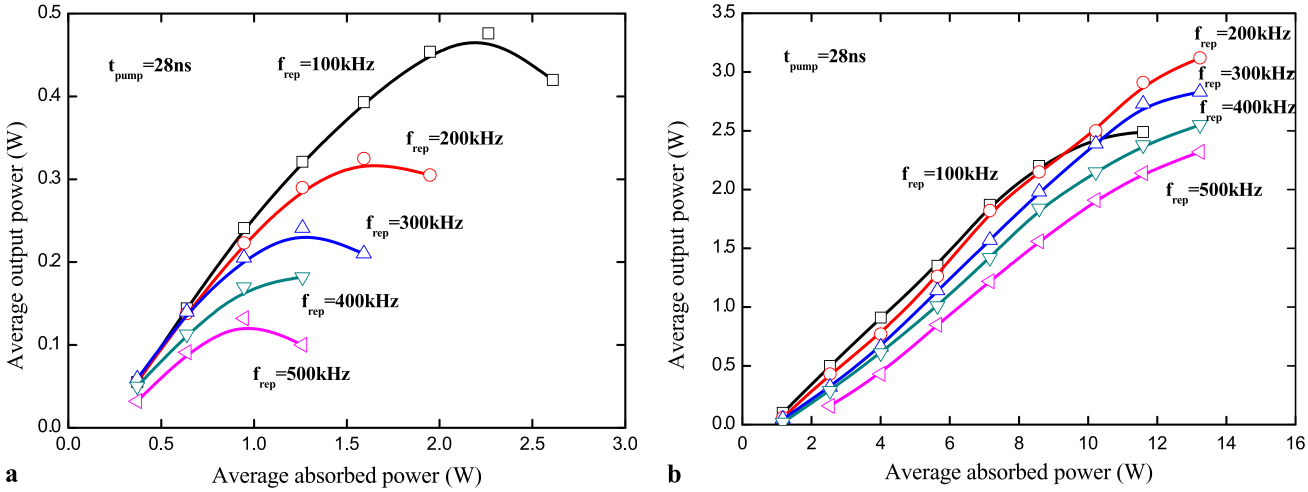

Fig. 4 Output performances without (**a**) and with (**b**) the diamond heat spreader for repetition rates in the range of 100–500 kHz

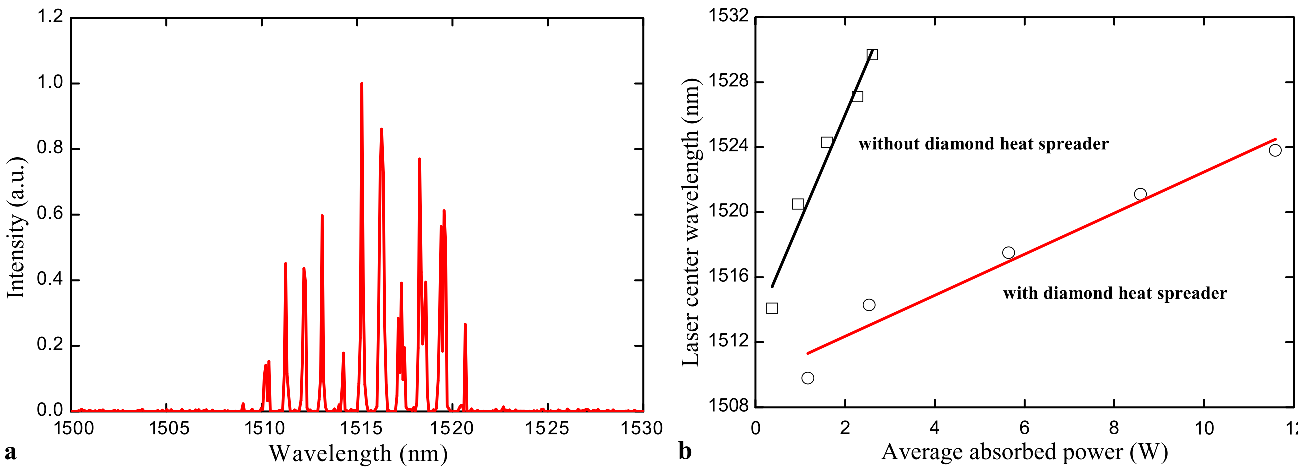

Fig. 5 (**a**) Lasing spectrum with the heat spreader under an average absorbed power of 2.5 W at a repetition rate of 100 kHz. (**b**) Dependence of the red-shift on the absorbed pump power for the laser operation without and with the heat spreader at a repetition rate of 100 kHz

can be seen that the redshift measured for the laser without using the heat spreader is considerably larger than the result with the heat spreader. This substantial difference also confirms the local heating to be considerably improved by use of the diamond heat spreader.

The temporal behavior of the laser output was recorded with a LeCrory digital oscilloscope (Wave pro 7100, 10 G samples/s, 1 GHz bandwidth). Figure 6 shows the input and output pulse trains as well as the extended pulse shape of the single pulse for the result obtained with an average absorbed power of 2.5 W at a repetition rate of 200 kHz. It can be seen that the time delay of the output pulse with respect to the input pulse is generally less than a few nanoseconds. The characteristics of the small delay comes from the advantage of the in-well pumping scheme. The peak-to-peak instability was experimentally found to arise from the instability of the pump beam. On the whole, the peak-to-peak fluctuation was generally within ±5 %. Finally it is worthwhile to mention that the present gain chip was designed for the high-peak-power operation and could not be used in the CW regime. We currently undertake a design for the gain chip to be applicable for the high-peak-power and CW operations.

4 Summary

In summary, we have demonstrated a high-repetition-rate (>100 kHz) nanosecond eye-safe AlGaInAs laser at 1525 nm with an Yb-doped pulsed fiber amplifier as a pump source. A diamond heat spreader bonded to the gain chip was employed to reach an efficient heat removal. With a pump power of 13.3 W, the maximum average output powers at the repetition rates of 200 kHz and 500 kHz were found to be up to 3.12 W and 2.32 W, respectively. Correspondingly, the maximum peak powers at the repetition

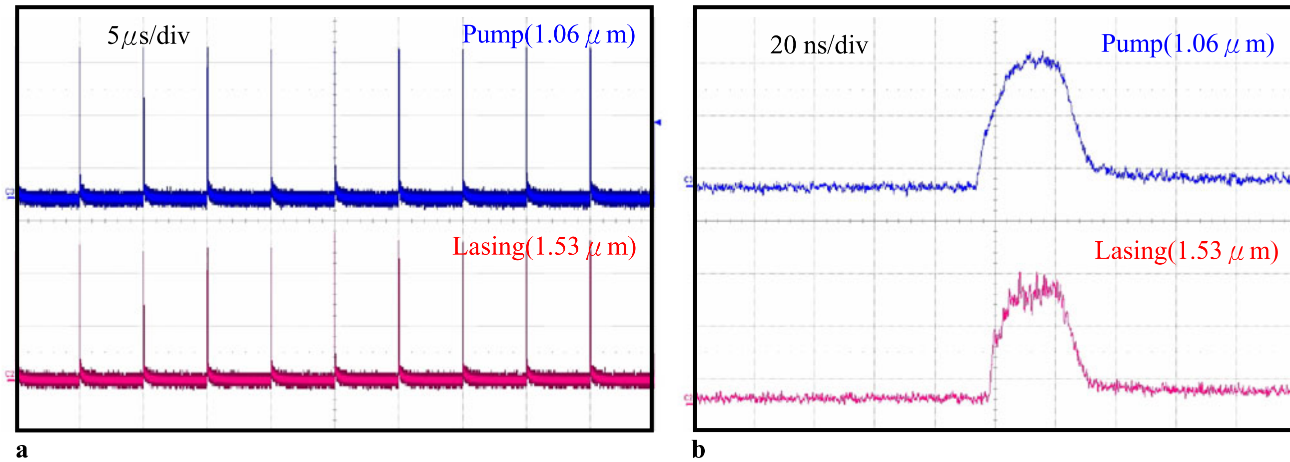

Fig. 6 (**a**) Oscilloscope trace of a train of pump and output pulses obtained with an average absorbed power of 2.5 W at a repetition rate of 200 kHz. (**b**) Expanded shapes of a single pulse

rates of 200 kHz and 500 kHz are 560 W and 170 W, respectively. To the best of our knowledge, this is the highest frequency achieved in the pulsed eye-safe lasers with the average output powers higher than 2 W.

Acknowledgements The authors gratefully acknowledge various AlGaInAs/InP gain chips from TrueLight Corporation. The authors also thank the National Science Council for their financial support of this research under Contract No. NSC-100-2628-M-009-001-MY3.

References

1. P. Černý, H. Jelínkova, P. Zverev, T.T. Basiev, Prog. Quantum Electron. **28**, 113 (2004)
2. S.H. Ding, X.Y. Zhang, Q.P. Wang, F.F. Su, P. Jia, S.T. Li, S.Z. Fan, J. Chang, S.S. Zhang, Z.J. Liu, IEEE J. Quantum Electron. **42**, 927 (2006)
3. Y.F. Chen, Opt. Lett. **29**, 2632 (2004)
4. J.T. Murray, R.C. Powell, D. Smith, W. Austin, R.A. Stolzenberger, Opt. Lett. **20**, 1017 (1995)
5. A. Agnesi, S. Dell'Acqua, G. Reali, Appl. Phys. B **70**, 751 (2000)
6. Y.F. Chen, S.W. Chen, Y.C. Chen, Y.P. Lan, S.W. Tsai, Appl. Phys. B **77**, 493 (2003)
7. H.T. Huang, J.L. He, X.L. Dong, C.H. Zuo, B.T. Zhang, G. Qiu, Z.K. Liu, Appl. Phys. B **90**, 43 (2008)
8. S. Kück, K. Petermann, U. Pohlmann, U. Schönhoff, G. Huber, Appl. Phys. B **58**, 153 (1994)
9. N.V. Kuleshov, A.A. Lagatsky, A.V. Podlipensky, V.P. Mikhailov, A.A. Kornienko, E.B. Dunina, S. Hartung, G. Huber, J. Opt. Soc. Am. B **15**, 1205 (1998)
10. I. Sokólska, E. Heumann, S. Kück, T. Łukasiewicz, Appl. Phys. B **71**, 893 (2000)
11. A. Sennaroglu, Prog. Quantum Electron. **26**, 287 (2002)
12. A.C. Tropper, H.D. Foreman, A. Garnache, K.G. Wilcox, S.H. Hoogland, J. Phys. D **37**, R75 (2004)
13. M. Kuznetsov, F. Hakimi, R. Sprague, A. Mooradian, IEEE Photonics Technol. Lett. **9**, 1063 (1997)
14. C.E. Zah, R. Bhat, B.N. Pathak, F. Favire, W. Lin, M.C. Wang, N.C. Andreadakis, D.M. Hwang, M.A. Koza, T.P. Lee, Z. Wang, D. Darby, D. Flanders, J.J. Heieh, IEEE J. Quantum Electron. **30**, 511 (1994)
15. J.P. Donnelly, J.N. Walpole, S.H. Groves, R.J. Bailey, L.J. Missaggia, A. Napoleone, R.E. Reeder, C.C. Cook, IEEE Photonics Technol. Lett. **10**, 1377 (1998)
16. J. Minch, S.H. Park, T. Keating, S.L. Chuang, IEEE J. Quantum Electron. **35**, 771 (1999)
17. S.R. Šelmić, G.A. Evans, T.M. Chou, J.B. Kirk, J.N. Walpole, J.P. Donnelly, C.T. Harris, L.J. Missaggia, IEEE Photonics Technol. Lett. **14**, 890 (2002)
18. J.C.L. Yong, J.M. Rorison, I.H. White, IEEE J. Quantum Electron. **38**, 1553 (2002)
19. N. Nishiyama, C. Caneau, B. Hall, G. Guryanov, M.H. Hu, X.S. Liu, M.-J. Li, R. Bhat, C.E. Zah, IEEE J. Sel. Top. Quantum Electron. **11**, 990 (2005)
20. H. Lindberg, A. Larsson, M. Strassner, Opt. Lett. **30**, 2260 (2005)
21. J. Rautiainen, J. Lyytikäinen, A. Sirbu, A. Mereuta, E. Kapon, O.G. Okhotnikov, Opt. Express **16**, 21881 (2008)
22. S.C. Huang, H.L. Chang, K.W. Su, A. Li, S.C. Liu, Y.F. Chen, K.F. Huang, Appl. Phys. B **94**, 483 (2009)
23. H.L. Chang, S.C. Huang, Yi-Fan Chen, K.W. Su, Y.F. Chen, K.F. Huang, Opt. Express **17**, 11409 (2009)
24. M.Y.A. Raya, S.R.J. Brueck, M. Osinsky, C.F. Schaus, J.G. Mcinery, T.M. Brennan, B.E. Hammons, IEEE J. Quantum Electron. **26**, 1500 (1989)
25. M.Y.A. Raya, S.R.J. Brueck, M.O. Scully, C. Lee, Phys. Rev. A **44**, 4599 (1991)
26. M. Schmid, S. Benchabane, F. Torabi-Goudarzi, R. Abram, A.I. Ferguson, E. Riis, Appl. Phys. Lett. **84**, 4860 (2004)
27. J.M. Hopkins, S.A. Smith, C.W. Jeon, H.D. Sun, D. Burns, S. Calvez, M.D. Dawson, T. Jouhti, M. Pessa, Electron. Lett. **40**, 30 (2004)
28. H. Lindberg, A. Strassner, E. Gerster, A. Larsson, Electron. Lett. **40**, 601 (2004)
29. V.-M. Korpijärvi, T. Leinonen, J. Puustinen, A. Härkönen, M.D. Guina, Opt. Express **18**, 25633 (2010)